

VALISENS: A Validated Innovative Multi-Sensor System for Cooperative Automated Driving

Lei Wan^{1,4}, Prabesh Gupta², Andreas Eich², Marcel Kettelgerdes³, Hannan Ejaz Keen¹,
Michael Klöppel-Gersdorf³, and Alexey Vinel⁴

Abstract—Perception is a core capability of automated vehicles and has been significantly advanced through modern sensor technologies and artificial intelligence. However, perception systems still face challenges in complex real-world scenarios. To improve robustness against various external factors, multi-sensor fusion techniques are essential, combining the strengths of different sensor modalities. With recent developments in Vehicle-to-Everything (V2X) communication, sensor fusion can now extend beyond a single vehicle to a cooperative multi-agent system involving Connected Automated Vehicle (CAV) and intelligent infrastructure. This paper presents VALISENS, an innovative multi-sensor system distributed across multiple agents. It integrates onboard and roadside LiDARs, radars, thermal cameras, and RGB cameras to enhance situational awareness and support cooperative automated driving. The thermal camera adds critical redundancy for perceiving Vulnerable Road User (VRU), while fusion with roadside sensors mitigates visual occlusions and extends the perception range beyond the limits of individual vehicles. We introduce the corresponding perception module built on this sensor system, which includes object detection, tracking, motion forecasting, and high-level data fusion. The proposed system demonstrates the potential of cooperative perception in real-world test environments and lays the groundwork for future Cooperative Intelligent Transport Systems (C-ITS) applications.

I. INTRODUCTION

The transportation system is undergoing a significant revolution, from isolated, manually operated vehicles and infrastructure toward a highly digitalized, intelligent, and connected ecosystem. At the core of this evolution are Cooperative Intelligent Transport Systems (C-ITS), which integrate Connected Automated Vehicle (CAV)s with intelligent infrastructure. These components are increasingly equipped with advanced sensors, high-performance computing units, and Vehicle-to-Everything (V2X) communication units, enabling them to perceive their surroundings and exchange data in real time. This shared situational awareness improves both autonomous navigation and infrastructure-supported transportation management.

*This research is financially supported by the German Federal Ministry for Economic Affairs and Climate Action (BMWK) under grant number FKZ 19A22009F (VALISENS).

¹XITASO GmbH, Austraße 35, 86153 Augsburg, Germany {lei.wan,hannan.keen}@xitaso.com

²LiangDao GmbH, Rosa-Bavarese-Str. 3, 80639 Munich, Germany {prabesh.gupta,andreas.eich}@liangdao.de

³Fraunhofer IVI, Institute for Transportation and Infrastructure Systems, Zeunerstr. 38, 01069 Dresden, Germany {michael.kloeppe,marcel.kettelgerdes}@ivi.fraunhofer.de

⁴Karlsruhe Institute of Technology, Kaiserstr. 89, 76133 Karlsruhe alexey.vinel@kit.edu

To achieve robust perception, CAVs typically rely on a combination of heterogeneous sensors, including LiDAR, radar, and RGB cameras [1]. LiDAR provides accurate 3D spatial measurements, radar offers robustness in adverse weather conditions, and RGB cameras contribute rich semantic information. Through multi-sensor fusion, vehicles can maintain reliable perception across varying environment, such as different lighting or weather conditions. However, the perception capabilities of an individual vehicle remain constrained in complex traffic environments, particularly due to limited sensing range and occlusions caused by other objects [2]. Recent advancements in V2X communication have made it possible to extend perception beyond the individual vehicle by enabling the sharing of sensor data among vehicles and infrastructure [3]. This cooperative perception paradigm significantly enhances the detection range and mitigates the impact of visual occlusions, contributing to improved safety and traffic efficiency. As a result, a dynamic, decentralized sensor network can be established, comprising multiple sensor-equipped entities, that supports a comprehensive and continuously updated understanding of the surrounding environment.

This paper presents VALISENS, an innovative and integrated sensor system designed to support cooperative automated driving. The system combines on-board and roadside sensing units, including LiDARs, radars, RGB cameras, and thermal cameras, to enhance perception capabilities in complex urban environments. Compared to conventional in-vehicle sensor systems, the inclusion of thermal cameras provides additional benefits for detecting and protecting VRUs, particularly in low-visibility conditions. Furthermore, the V2X-enabled architecture facilitates the extension of the sensor network beyond individual vehicles, enabling flexible and scalable collaborative perception.

To evaluate the proposed system, a perception module is developed that comprises components of object detection, tracking, and motion prediction. These modules are deployed and validated in real-world test environments using two sensor-equipped vehicles and infrastructure-based sensor units. The evaluation demonstrates the effectiveness of the VALISENS system in improving situational awareness and enhancing road safety, especially for VRU protection.

A. Related Work

1) *Communication*: Communication plays a central role in C-ITS, enabling real-time cooperation between vehicles, infrastructure, and other road users. Dedicated Short-



Fig. 1: Sensor layout at the SmartIntersection in Dresden. The red circle shows the detection range of the LiDAR, the yellow ellipses show the detection area of the single radar sensors, and the blue (thermal) and green (thermal+RGB) polygons show the area covered by cameras.

Range Communication (DSRC) and cellular networks are two primary technologies used for message exchange [4]. DSRC allows direct communication between devices with low latency, making it suitable for safety-critical applications [5]. However, its limited bandwidth restricts the range of supported services. To address these limitations, Cellular-V2X (C-V2X) has emerged as a complementary technology, offering greater bandwidth and supporting data-intensive applications such as cooperative perception. To enhance interoperability and deployment flexibility, dual-mode V2X modules supporting both DSRC and C-V2X are now commercially available [6]. The system proposed in this paper uses such a dual compatible V2X stack to facilitate testing of both communication protocols and to ensure interoperability between heterogeneous vehicles of different manufacturers.

2) *Perception*: Perception for autonomous vehicles has been extensively studied in recent years, evolving from single-sensor approaches to multi-sensor fusion systems, and from isolated in-vehicle or roadside sensors to dynamic, multi-agent sensor networks. In-vehicle sensor systems have been the foundation of many large-scale vehicle-perspective datasets such as KITTI [7], nuScenes [8], and Waymo Open Dataset [9], supporting a wide range of perception tasks including object detection, tracking, semantic segmentation, and motion prediction. Recently, there has been a growing interest in roadside sensor systems, as reflected in the increasing number of roadside perception data sets such as Rope3D [10], A9-Dataset [11], and R-LiViT [12]. The integration of sensor data from both vehicles and infrastructure has led to the development of collaborative perception datasets such as DAIR-V2X [13], V2X-Seq [14], V2V4Real [15], and V2X-Real [16]. Collectively, these datasets underscore the growing focus on multi-agent sensor networks that incorporate diverse modalities across vehicles and infrastructure.

In such networks, data fusion is a key component for generating a unified and consistent understanding of the environment. Fusion strategies are commonly categorized into early fusion [17], intermediate fusion [18], and late fusion [19]. Among these, late fusion, where object-level information is exchanged and aggregated, has emerged as the most practical approach for deployment. It is model- and modality-agnostic and significantly reduces bandwidth

requirements compared to early fusion, making it better aligned with the realistic constraints of V2X communication. The system proposed in this paper adopts a late fusion approach to enable modular perception across heterogeneous sensors and ensure compatibility with communication standards defined by European Telecommunications Standards Institute (ETSI).

3) *Sensor Condition Monitoring*: The performance of a multi-modal perception system is directly dependent on error-free operation and data integrity of the underlying sensor hardware. As compiled by Goelles et al. [20] and Secci et al. [21], especially in the case of optical sensors such as cameras and LiDAR, a multitude of failure mechanisms can, however, lead to severely degraded performance in terms of output data quality or even total system failure. Thus, common error sources include well-studied external effects, such as sensor blockage due to leaves and dirt [22], but also adverse weather conditions such as precipitation, fog or sun glare [23], [24]. In addition to external effects, internal failure or component degradation might occur over time, especially considering the demanding thermo-mechanical operating conditions in the automotive domain. Internal effects include electrical failures, such as dead pixels or broken components such as the processing unit or, in the case of the LiDAR, the laser diode [21], [20]. Furthermore, it could be shown that the sensor's optical receiver front end can be prone to degradation, expressed, for example, in intrinsic decalibration [25], [26] or loss of sharpness [27].

Considering the multitude of possible failure sources and their high criticality due to the potentially hazardous consequences in safety-critical automotive applications, condition monitoring of these sensors plays a crucial role in robust environmental perception. However, while there exist several works on the monitoring of external effects, such as weather conditions [28], [29], only a few focus on internal effects. Plus, existing works propose rather abstract monitoring concepts and frameworks than specific methods, which could be due to the lack of publicly available data in this domain, as noted by Goelles et al. [20]. Following that, extensive reliability testing of sensors constitutes a crucial part of the overall condition monitoring methodology [30].

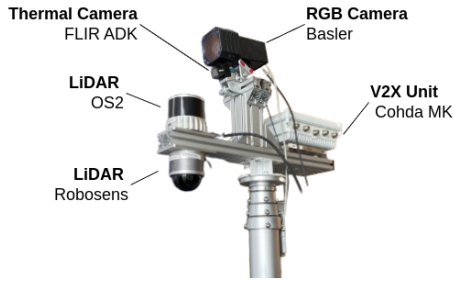


Fig. 2: Sensor configurations of the mobile sensor platform

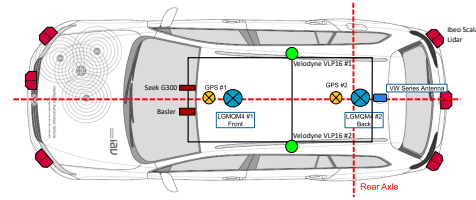
II. SYSTEM ARCHITECTURE

This section provides an overview of the proposed multi-agent sensor system and the core functionalities built upon it. Section II-A describes the sensor-equipped infrastructure and vehicle platforms. Sections II-B, II-C, and II-D present the key functional modules of the system, including environment perception, trajectory prediction, and sensor monitoring.

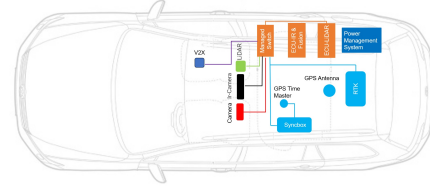
A. Overview

The overall system comprises both infrastructure and vehicles, each equipped with multiple sensors, computing units, and V2X communication stack, as detailed in the following sections. Intra-entity communication is handled using ROS2[31], while inter-entity communication, specifically between infrastructure and vehicles, is facilitated through V2X.

1) *Infrastructure systems*: Two test beds are utilized to support the sensor system. The primary test bed is located at a public intersection in Dresden, Germany (Zellescher Weg/Paradiesstraße). As Figure 1 shows, this site is equipped with six cameras (five thermal cameras and one dual-mode RGB/thermal camera), one LiDAR system (Ouster OS1 with 64 layers in below horizon configuration, complemented, in the blind-zone, by a Robosense BPearl), and one radar system featuring 4x4 MIMO capability. All roadside sensors are synchronized using a Network Time Protocol (NTP) server provided by the Road-Side Unit (RSU) and are calibrated to a shared intersection base link. For data processing, three NVIDIA Jetson AGX Orin devices and one Jetson AGX Xavier are deployed and connected to all sensor components via Ethernet. Communication with vehicles and back-end systems is facilitated by a Cohda MK6 RSU for V2X messaging and a Milesight UR75 5G router. A detailed description of this test bed can be found in [32]. The second test bed is located in Ingolstadt and consists of 22 sensor masts. The western part of the test bed is characterized by a heterogeneous sensor setup, where only three of the eleven masts are equipped with V2X communication. In contrast, the eastern part is characterized by a homogeneous sensor and communication setup, consisting of LiDAR systems (the same setup as in the Dresden test bed), RGB cameras, and Cohda MK6. A detailed description of the test bed, including V2X measurements, can be found in [33]. To complement the fixed infrastructure, a mobile sensor platform, referred to as the Rover, is also employed. The Rover, shown in Figure



(a) Sensor positions on test vehicle One. The LGMQM4 antennas are used to provide 5G and V2X connectivity.



(b) Sensor positions and wiring on test vehicle Two.

Fig. 3: Sensor configurations on test vehicles used in the experiments.

2, is equipped with one RGB camera, one thermal camera, and the same LiDAR configuration as used in the fixed test beds. It is also equipped with a Cohda MK6 RSU for V2X communication, a Jetson AGX Orin and an x86_64-based computing unit with an NVIDIA RTX 4060 GPU for real-time data processing.

2) *Vehicle systems*: In parallel to the infrastructure setup, two sensor-equipped vehicles are used for testing and evaluation. As Figure 3 shows, both vehicles feature a dual-camera setup consisting of a Seek infrared camera and a Basler RGB camera, as well as a Cohda MK6 On-Board Unit (OBU) for V2X communication. Vehicle One is outfitted with two Velodyne VLP-16 LiDARs mounted on the roof and six IBEO Scala LiDARs positioned on the front and rear bumpers. It also includes a NovAtel PowerPak7-E1 Global Navigation Satellite System (GNSS) with integrated IMU for high precision localization. The onboard computing platform comprises three x86_64-based units, one of which is equipped with an NVIDIA RTX 2000 GPU to enable real-time AI processing. All onboard sensors are synchronized using an NTP server and calibrated relative to the Velodyne LiDAR. A prior version of this vehicle configuration is described in [34]. Vehicle Two is equipped with an InnovizOne LiDAR mounted on the roof and a DTC xNAV650 (GPS/RTK) inertial navigation system. For onboard processing, it features two Jetson AGX Orin devices, one dedicated to image processing and the other to LiDAR-data processing. The sensors in Vehicle Two are synchronized via a Precision Time Protocol (PTP) server and calibrated with respect to the LiDAR system.

B. Environmental perception concept

The concept of environmental perception is modularized by the sensor modality, as illustrated in Figure 4. Each

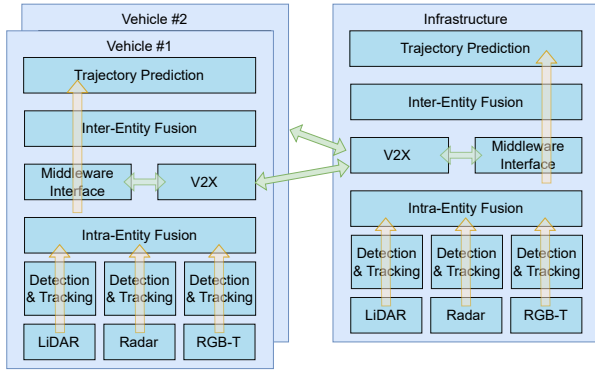


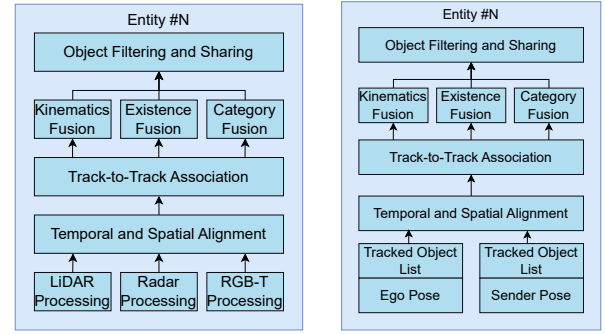
Fig. 4: Software architecture overview of environmental perception.

modality independently delivers a list of detected and tracked objects to downstream modules, enabling the seamless integration of heterogeneous sensors. The perception outputs are first aggregated by the intra-entity fusion node, which combines data from multiple sensors within the same platform. Subsequently, the inter-entity fusion node integrates information across different agents (e.g., vehicles and infrastructure). The fused object-level data is then passed to the trajectory prediction module to support cooperative automated driving.

1) *LiDAR*: In the proposed system, LiDAR data is processed using a LiangDao in-house developed AI-based perception algorithms to enable both short- and long-range detection and tracking of relevant traffic participants. The output includes 3D bounding boxes with associated semantic labels, tracking ID, 3D position, 3D dimensions, velocity, and heading angle. LiDARs are deployed across both infrastructure and vehicle platforms in various configurations. In setups involving multiple LiDAR units, point clouds are fused prior to perception module using an early fusion approach, thereby enabling a more complete and consistent view of the environment.

2) *Radar*: Multiple radar units are installed on infrastructure, each oriented toward different road directions to ensure comprehensive coverage of the intersection area. The outputs of the single radar sensors are fused by an in-house algorithm by smartmicro, which returns object lists represented in a Bird’s-Eye View (BEV), excluding height information (z-dimension). To enable fusion with LiDAR data, radar object lists undergo post-processing by assigning a default height value, thereby reconstructing the data into full 3D coordinates.

3) *RGB-T*: In the proposed architecture, RGB and thermal data are processed independently and fused using a late fusion strategy; even if one camera failed, the RGB-T module still delivers a reliable result. Here, we utilize the YOLO framework [35] as the detector for each camera, producing a 2D object bounding box in the image plane. To aggregate results from multiple cameras, the bounding boxes are first projected to the core camera image plane and then fused by Non-Maximum Suppression (NMS) [36] operation. The resulting fused bounding boxes are then passed to a 2D



(a) Intra-entity fusion

(b) Inter-entity fusion

Fig. 5: Schematic diagrams of intra-entity and inter-entity fusion approaches

multi-object tracking node, which employs the ByteTrack algorithm [37] to track objects across frames in real time.

4) *Intra-Entity Fusion*: To produce a unified and consistent perception output, all modality-specific results are forwarded to the intra-entity fusion node. The proposed system employs a late fusion approach that integrates object-level information from multiple sensors. Each sensor module provides a list of tracked objects, which are merged into a unified 3D representation containing 3D position, 3D dimensions, velocity, class label, confidence, and tracking ID.

As shown in Fig. 6, the fusion module utilizes a track-to-track fusion algorithm [38], which consists of three main stages: alignment, association, and fusion. In the *alignment stage*, the object data is spatially transformed from the local coordinate system of each sensor into the vehicle’s base-link coordinate. Temporal alignment is achieved using a constant velocity model to project object states to a common timestamp. Once aligned, *association stage* is performed using a combination of Euclidean distance and Intersection-over-Union (IoU) thresholds to match corresponding detections across modalities. In *fusion stage*, associated objects are then fused using an adapted Kalman filter, where each observation is treated as a measurement to update the global object state and covariance. In addition to position and velocity, the fusion process also incorporates object classification and shape. Class labels from camera are given higher weight due to their superior semantic accuracy, while LiDAR-based estimates are prioritized for object shape due to their precise 3D measurement. Radar-based velocity estimates are given a higher weight because of their direct Doppler-based measurement mechanism, which provides accurate motion information. Before publishing the final fused output, object existence probabilities are recalculated, and only those exceeding a predefined confidence threshold are retained.

5) *Communication and Inter-Entity Fusion*: The proposed system adopts a late fusion strategy for inter-entity fusion, in alignment with the communication standards defined by ETSI. Specifically, the system utilizes the Collective Perception Message (CPM) [39] message to transmit perception

data, which include the pose of the ego vehicle along with a list of tracked objects. In the implemented architecture, the output of the intra-entity fusion module is used to generate CPM messages, which are then broadcast via the V2X communication stack. Other entities within the communication range receive and decode the CPM, extracting both the sender’s pose and its associated perception results. To fuse data from external agents, the same fusion strategy described in Section II-B.4 is applied. Received objects are first transformed from the sender’s coordinate frame into the ego vehicle’s frame. They are then spatially and temporally aligned, associated with locally perceived objects, and fused using the track-to-track fusion pipeline, as shown in Figure 6. This process enables robust and seamless cooperation among heterogeneous agents, resulting in a continuous and unified understanding of the surrounding environment.

C. Trajectory prediction concept

In addition to detection and tracking, forecasting the future behavior of road users is essential for cooperative automated driving. Trajectory prediction improves situational awareness by estimating actions such as whether a pedestrian intends to cross the street or stay on the sidewalk, which is a critical information for both vehicle decision making and infrastructure-based alert systems. In the proposed system, as shown in Figure 6a, the trajectory prediction module receives tracked objects as input, enriched with map data describing the local intersection geometry. Using this combined information, the module predicts future trajectories for all perceived dynamic agents in the scene. For prediction, the system employs the MTR++ framework [40], a transformer-based architecture that encodes both agents’ historical motion and semantic map features into a unified latent representation. This representation is then decoded to produce multi-step trajectory forecasts for each road user. The predicted trajectories are subsequently analyzed for potential collision risks. Specifically, the system evaluates whether the future paths of any agent are likely to intersect. Trajectories considered safety critical are flagged and visualized using a color-coded scheme, enabling both automated vehicles and infrastructure systems to respond proactively to emerging hazards.

D. Sensor Condition Monitoring Concept

In order to ensure reliable perception performance and resilience with respect to failure sources introduced in Sec. I, a sensor condition monitoring module is developed and evaluated for automotive grade camera sensors in the test bed Ingolstadt. For that, extensive reliability testing is conducted in order to identify potential internal failures in addition to well-studied external effects. Initial thermal cycling tests, conducted under the LV124 automotive test standard for accelerated aging [41], did not show a significant gradual degradation of optical performance in the form of loss of sharpness or decalibration. Hence, the condition monitoring concept focuses on anomaly detection of permanent and non-permanent external and internal faults, such as adverse

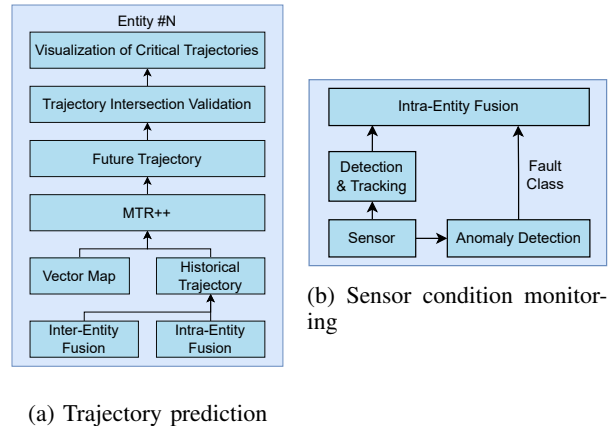


Fig. 6: Schematic diagrams of trajectory prediction and sensor condition monitoring approaches

TABLE I: Communication Performance Indicators

Modality	Measurements
5G Dresden test bed	UL: 80 Mbps, DL: 65 Mbps
5G Vehicle One	UL: 65 Mbps, DL: 0.6 Gbps
V2X Dresden test bed	Max. range: ≥ 1 km

weather conditions, blockage by dirt, ice, or fogging, and permanent imager faults.

Therefore, the dataset generated from reliability testing is augmented by simulated and physically induced errors. Based on that, a classifier is trained on the respective raw image data in order to predict the camera state in the form of dedicated fault classes which can be communicated to higher-level fusion entities, as illustrated in Fig. 6b.

III. RESULTS

This section presents a quantitative evaluation of the system’s communication performance and perception capabilities.

A. Communication Performance

Table I summarizes key communication performance indicators. Up- (UL) and Download (DL) were measured using iperf3. The high DL values for the vehicle were achieved by using Multi-WAN, i.e. the router is connected to and uses two mobile communication providers in parallel. V2X communication range was evaluated from Cooperative Awareness Messages (CAMs) [42], which were received at the target intersection. As these messages do not hop, the location information within the messages can be used to evaluate the maximum communication range. Still, ranges as reported here are only possible under line-of-sight conditions and present a best case. Under adverse conditions, e.g., a truck blocking line-of-sight, communication ranges can drop significantly.

B. Perception Performance

We have quantitatively evaluated the perception module using data collected by the Rover (a mobile sensor platform). The dataset comprises multi-modal sensor data from three

different intersections, recorded during both daytime and nighttime conditions. It includes 10,000 annotated LiDAR frames and 2,400 annotated RGB-Thermal frames [12], covering various categories such as cars, trucks, buses, trams, motorcycles, cyclists, and pedestrians. The dataset is particularly rich in VRUs, containing over 95,000 pedestrian annotations and more than 10,000 cyclist annotations.

TABLE II: LiDAR object detection results on mobile sensor platform.

Method	AP ₅₀		
	Car	Pedestrian	Cyclist
PointPillars [43]	58.38	23.07	30.11
PointRCNN [44]	31.58	4.62	11.76
PV-RCNN [45]	56.19	19.79	28.43

Object detection performance was assessed using the Average Precision (AP) metric with an Intersection over Union (IoU) threshold of 0.5. Table II reports the LiDAR-based detection results for cars, pedestrians, and cyclists. Among the evaluated methods, PointPillars [43] delivered the highest precision across all categories, confirming its strong performance in LiDAR-based detection tasks. Table III presents the results for RGB-Thermal detection. The YOLOv8 model [46] achieved the best overall performance, attaining an AP@50 score of 63.02. As the results show, combining RGB and thermal data achieves better results for pedestrian detection compared to using either modality alone, underscoring its potential to enhance VRU detection.

Due to the limited availability of annotated data covering all involved entities (two vehicles and infrastructure components), comprehensive quantitative evaluations of the complete cooperative system are beyond the scope of this paper. Future research will address this limitation by collecting and annotating a large-scale data set that encompasses all relevant entities of the system.

IV. CONCLUSION

This paper presents an innovative multi-sensor system that integrates both onboard and roadside sensors with a comprehensive perception module. By fusing data from these diverse sources, CAVs achieve a more complete understanding of their surroundings while maintaining robustness against external interference, such as weather and lighting conditions. The incorporation of roadside sensors addresses a key challenge in autonomous driving by eliminating visual occlusions and significantly extending the vehicle’s perception range. As a result, vehicles operate with enhanced situational awareness, and transportation authorities benefit from more precise traffic monitoring, enabling the deployment of advanced traffic management systems. Our implementation of this architecture in real-world test field and vehicles validates its effectiveness and establishes a strong foundation for future C-ITS applications.

TABLE III: RGB-T object detection results on mobile sensor platform, AR_{per}¹⁰⁰ denotes average recall for pedestrians considering up to 100 detections.

Model	Modality	Day		Night	
		AP ₅₀	AR _{per} ¹⁰⁰	AP ₅₀	AR _{per} ¹⁰⁰
Faster R-CNN [47]	RGB	61.32	43.44	48.76	38.30
	Thermal	40.60	27.91	39.18	25.55
	RGB+T	53.95	46.74	41.93	44.67
YOLOv8 [46]	RGB	63.02	46.39	49.85	37.76
	Thermal	50.11	33.39	49.04	31.83
	RGB+T	59.93	50.42	53.26	45.34
RT-DETR [48]	RGB	59.67	40.68	54.60	34.15
	Thermal	50.70	31.84	50.48	28.74
	RGB+T	58.78	44.93	58.78	41.14

REFERENCES

- [1] X. Zhang, Y. Gong, J. Lu, J. Wu, Z. Li, D. Jin, and J. Li, “Multi-modal fusion technology based on vehicle information: A survey,” *IEEE Transactions on Intelligent Vehicles*, vol. 8, no. 6, pp. 3605–3619, 2023.
- [2] L. Wan, H. E. Keen, and A. Vinel, “The components of collaborative joint perception and prediction—a conceptual framework,” *arXiv preprint arXiv:2501.15860*, 2025.
- [3] L. Wan, J. Zhao, A. Wiedholz, M. Bied, M. M. de Lucena, A. D. Jagtap, A. Festag, A. A. Fröhlich, H. E. Keen, and A. Vinel, “Systematic literature review on vehicular collaborative perception—a computer vision perspective,” *arXiv preprint arXiv:2504.04631*, 2025.
- [4] Y. Jin, X. Liu, and Q. Zhu, “Dsrc and c-v2x comparison for connected and automated vehicles in different traffic scenarios,” *arXiv preprint arXiv:2203.12553*, 2022.
- [5] V. Mannoni, V. Berg, S. Sesia, and E. Perraud, “A comparison of the v2x communication systems: Its-g5 and c-v2x,” in *2019 IEEE 89th Vehicular Technology Conference (VTC2019-Spring)*. IEEE, 2019, pp. 1–5.
- [6] K. Z. Ghafoor, M. Guizani, L. Kong, H. S. Maghdid, and K. F. Jasim, “Enabling efficient coexistence of dsrc and c-v2x in vehicular networks,” *IEEE Wireless Communications*, vol. 27, no. 2, pp. 134–140, 2020.
- [7] A. Geiger, P. Lenz, C. Stiller, and R. Urtasun, “Vision meets robotics: The kitti dataset,” *The international journal of robotics research*, vol. 32, no. 11, pp. 1231–1237, 2013.
- [8] H. Caesar, V. Bankiti, A. H. Lang, S. Vora, V. E. Liong, Q. Xu, A. Krishnan, Y. Pan, G. Baldan, and O. Beijbom, “nusenes: A multimodal dataset for autonomous driving,” in *Proceedings of the IEEE/CVF conference on computer vision and pattern recognition*, 2020, pp. 11 621–11 631.
- [9] P. Sun, H. Kretzschmar, X. Dotiwalla, A. Chouard, V. Patnaik, P. Tsui, J. Guo, Y. Zhou, Y. Chai, B. Caine, *et al.*, “Scalability in perception for autonomous driving: Waymo open dataset,” in *Proceedings of the IEEE/CVF conference on computer vision and pattern recognition*, 2020, pp. 2446–2454.
- [10] X. Ye, M. Shu, H. Li, Y. Shi, Y. Li, G. Wang, X. Tan, and E. Ding, “Rope3d: Theroadside perception dataset for autonomous driving and monocular 3d object detection task,” *arXiv preprint arXiv:2203.13608*, 2022.
- [11] W. Zimmer, C. Creß, H. T. Nguyen, and A. C. Knoll, “Tumtraf intersection dataset: All you need for urban 3d camera-lidar roadside perception,” in *2023 IEEE 26th International Conference on Intelligent Transportation Systems (ITSC)*, 2023, pp. 1030–1037.
- [12] J. Mirlach, L. Wan, A. Wiedholz, H. E. Keen, and A. Eich, “R-livit: A lidar-visual-thermal dataset enabling vulnerable road user focused roadside perception,” *arXiv preprint arXiv:2503.17122*, 2025.
- [13] H. Yu, Y. Luo, M. Shu, Y. Huo, Z. Yang, Y. Shi, Z. Guo, H. Li, X. Hu, J. Yuan, and Z. Nie, “Dair-v2x: A large-scale dataset for vehicle-infrastructure cooperative 3d object detection,” in *Proceedings of the IEEE/CVF Conference on Computer Vision and Pattern Recognition*, 2022, pp. 21 361–21 370.

- [14] H. Yu, W. Yang, H. Ruan, Z. Yang, Y. Tang, X. Gao, X. Hao, Y. Shi, Y. Pan, N. Sun, J. Song, J. Yuan, P. Luo, and Z. Nie, "V2x-seq: A large-scale sequential dataset for vehicle-infrastructure cooperative perception and forecasting," in *Proceedings of the IEEE/CVF Conference on Computer Vision and Pattern Recognition*, 2023.
- [15] R. Xu, X. Xia, J. Li, H. Li, S. Zhang, Z. Tu, Z. Meng, H. Xiang, X. Dong, R. Song, H. Yu, B. Zhou, and J. Ma, "V2v4real: A real-world large-scale dataset for vehicle-to-vehicle cooperative perception," in *The IEEE/CVF Computer Vision and Pattern Recognition Conference (CVPR)*, 2023.
- [16] H. Xiang, Z. Zheng, X. Xia, R. Xu, L. Gao, Z. Zhou, X. Han, X. Ji, M. Li, Z. Meng, et al., "V2x-real: a large-scale dataset for vehicle-to-everything cooperative perception," in *European Conference on Computer Vision*. Springer, 2024, pp. 455–470.
- [17] A. N. Ahmed et al., "A joint perception scheme for connected vehicles," in *2022 Proceedings of IEEE Sensors*. Dallas, TX, USA: IEEE, Oct. 2022, pp. 1–4, doi: 10.1109/SENSOR52175.2022.9967271.
- [18] J. Guo, D. Carrillo, Q. Chen, Q. Yang, S. Fu, H. Lu, and R. Guo, "Slim-FCP: Lightweight-feature-based cooperative perception for connected automated vehicles," *IEEE Internet of Things Journal*, vol. 9, no. 17, pp. 15 630–15 638, 2022.
- [19] R. Xu, W. Chen, H. Xiang, X. Xia, L. Liu, and J. Ma, "Model-agnostic multi-agent perception framework," in *2023 IEEE International Conference on Robotics and Automation (ICRA)*, 2023, pp. 1471–1478.
- [20] T. Goelles, B. Schlager, and S. Muckenhuber, "Fault detection, isolation, identification and recovery (fdiir) methods for automotive perception sensors including a detailed literature survey for lidar," *Sensors (Basel, Switzerland)*, vol. 20, no. 13, p. 3662, 2020.
- [21] F. Secci and A. Ceccarelli, "On failures of rgb cameras and their effects in autonomous driving applications," in *2020 IEEE 31st International Symposium on Software Reliability Engineering*, M. Vieira, Ed. Piscataway, NJ: IEEE, 2020, pp. 13–24.
- [22] M. Trierweiler, P. Caldelas, G. Groninger, T. Peterseim, and C. Neumann, "Influence of sensor blockage on automotive lidar systems," in *2019 IEEE SENSORS*. IEEE, 102019, pp. 1–4.
- [23] C. Linnhoff, K. Hofrichter, L. Elster, P. Rosenberger, and H. Winner, "Measuring the influence of environmental conditions on automotive lidar sensors," *Sensors (Basel, Switzerland)*, vol. 22, no. 14, 2022.
- [24] T. Brophy, D. Mullins, A. Parsi, J. Horgan, E. Ward, P. Denny, C. Eising, B. Deegan, M. Glavin, and E. Jones, "A review of the impact of rain on camera-based perception in automated driving systems," *IEEE Access*, vol. 11, pp. 67 040–67 057, 2023.
- [25] B. Li, P. H. Chan, G. Baris, M. D. Higgins, and V. Donzella, "Analysis of automotive camera sensor noise factors and impact on object detection," *IEEE Sensors Journal*, vol. 22, no. 22, pp. 22 210–22 219, 2022.
- [26] M. Kettelgerdes, L. Bohm, and G. Elger, "Correlating intrinsic parameters and sharpness for condition monitoring of automotive imaging sensors," in *2021 5th International Conference on System Reliability and Safety (ICSRS)*. IEEE, 2021, pp. 298–306.
- [27] A. Pandey, D. Unruh, M. Kettelgerdes, B. Wunderle, and G. Elger, "Evaluation of thermally induced change in sharpness of automotive cameras by coupled thermo-mechanical and optical simulation," in *SPIE Digital Library Proceedings*. SPIE, 2023, pp. 147–153.
- [28] M. M. Dhananjaya, V. R. Kumar, and S. Yogamani, "Weather and light level classification for autonomous driving: Dataset, baseline and active learning," in *2021 IEEE International Intelligent Transportation Systems Conference (ITSC)*, 2021, pp. 2816–2821.
- [29] M. Kettelgerdes, N. Sarmiento, H. Erdogan, B. Wunderle, and G. Elger, "Precise adverse weather characterization by deep-learning-based noise processing in automotive lidar sensors," *Remote Sensing*, vol. 16, no. 13, 2024.
- [30] M. Kettelgerdes, T. Hirmer, T. Hillmann, H. Erdogan, B. Wunderle, and G. Elger, "Accelerated real-life testing of automotive lidar sensors as enabler for in-field condition monitoring," in *Tagungsband Symposium Elektronik und Systemintegration*, 2024, vol. 4, pp. 87–98.
- [31] S. Macenski, T. Foote, B. Gerkey, C. Lalancette, and W. Woodall, "Robot operating system 2: Design, architecture, and uses in the wild," *Science Robotics*, vol. 7, no. 66, p. eabm6074, 2022.
- [32] M. Klöppel-Gersdorf, F. Trauzettel, K. Koslowski, M. Peter, and T. Otto, "The fraunhofer ccit smart intersection," in *2021 IEEE International Intelligent Transportation Systems Conference (ITSC)*. IEEE, 2021, pp. 1797–1802.
- [33] R. Song, A. Festag, A. D. Jagtap, M. Bialdyga, Z. Yan, M. Otte, S. T. Sadashivaiah, and A. Knoll, "First mile: An open innovation lab for infrastructure-assisted cooperative intelligent transportation systems," in *2024 IEEE Intelligent Vehicles Symposium (IV)*. IEEE, 2024, pp. 1635–1642.
- [34] M. Klöppel-Gersdorf and T. Otto, "Evaluating message size of the collective perception message in real live settings," in *Proceedings of the 7th International Conference on Vehicle Technology and Intelligent Transport Systems - VEHITS*, INSTICC. SciTePress, 2021, pp. 554–561.
- [35] R. Khanam and M. Hussain, "Yolov11: An overview of the key architectural enhancements," *arXiv preprint arXiv:2410.17725*, 2024.
- [36] A. Neubeck and L. Van Gool, "Efficient non-maximum suppression," in *18th international conference on pattern recognition (ICPR'06)*, vol. 3. IEEE, 2006, pp. 850–855.
- [37] Y. Zhang, P. Sun, Y. Jiang, D. Yu, F. Weng, Z. Yuan, P. Luo, W. Liu, and X. Wang, "Bytetrack: Multi-object tracking by associating every detection box," in *European conference on computer vision*. Springer, 2022, pp. 1–21.
- [38] M. Aeberhard, S. Schlichtharle, N. Kaempchen, and T. Bertram, "Track-to-track fusion with asynchronous sensors using information matrix fusion for surround environment perception," *IEEE Transactions on Intelligent Transportation Systems*, vol. 13, no. 4, pp. 1717–1726, 2012.
- [39] ETSI, "ETSI TS 103 324 V2.1.1 (2023-06) Intelligent Transport Systems (ITS); Vehicular Communications; Basic Set of Applications; Collective Perception Service; Release 2," ETSI, Standard, June 2023.
- [40] S. Shi, L. Jiang, D. Dai, and B. Schiele, "Mtr++: Multi-agent motion prediction with symmetric scene modeling and guided intention querying," *IEEE Transactions on Pattern Analysis and Machine Intelligence*, vol. 46, no. 5, pp. 3955–3971, 2024.
- [41] BMW AG, AUDI AG, Volkswagen AG Porsche AG ff., "Elektrische und elektronische Komponenten in Kraftfahrzeugen bis 3,5t: Allgemeine Anforderungen, Prüfbedingungen und Prüfungen," 15.10.2009.
- [42] ETSI, "ETSI EN 302 637-2 V1.4.1 (2019-04) Intelligent Transport Systems (ITS); Vehicular Communications; Basic Set of Applications; Part 2: Specification of Cooperative Awareness Basic Service," ETSI, Standard, April 2019.
- [43] A. H. Lang, S. Vora, H. Caesar, L. Zhou, J. Yang, and O. Beijbom, "Pointpillars: Fast encoders for object detection from point clouds," in *Proceedings of the IEEE/CVF conference on computer vision and pattern recognition*, 2019, pp. 12 697–12 705.
- [44] S. Shi, X. Wang, and H. Li, "Pointrcnn: 3d object proposal generation and detection from point cloud," in *Proceedings of the IEEE/CVF conference on computer vision and pattern recognition*, 2019, pp. 770–779.
- [45] S. Shi, C. Guo, L. Jiang, Z. Wang, J. Shi, X. Wang, and H. Li, "Pv-rcnn: Point-voxel feature set abstraction for 3d object detection," in *Proceedings of the IEEE/CVF conference on computer vision and pattern recognition*, 2020, pp. 10 529–10 538.
- [46] G. Jocher, J. Qiu, and A. Chaurasia, "Ultralytics YOLO," Jan. 2023. [Online]. Available: <https://github.com/ultralytics/ultralytics>
- [47] S. Ren, K. He, R. Girshick, and J. Sun, "Faster r-cnn: Towards real-time object detection with region proposal networks," in *Advances in Neural Information Processing Systems*, C. Cortes, N. Lawrence, D. Lee, M. Sugiyama, and R. Garnett, Eds., vol. 28. Curran Associates, Inc., 2015.
- [48] Y. Zhao, W. Lv, S. Xu, J. Wei, G. Wang, Q. Dang, Y. Liu, and J. Chen, "Detrs beat yolos on real-time object detection," in *2024 IEEE/CVF Conference on Computer Vision and Pattern Recognition (CVPR)*, 2024, pp. 16 965–16 974.